JOURNAL

of

STEEL CASTINGS RESEARCH

CONTENTS

A Microscopic Study of the Bonding of Steel Foundry Sands by Clays 1

Grain of Solidifying Metal Refined by Vibration 7

The Solidification of Steel Castings 9

A Testing Machine for Blast Cleaning Abrasives 14

Abstracts of Fundamental Papers on Steel Casting Research 16

STEEL FOUNDERS' SOCIETY OF AMERICA

NUMBER 16 JANUARY, 1960

JOURNAL OF STEEL CASTINGS RESEARCH

Number 16 **January, 1960**

TECHNICAL RESEARCH COMMITTEE, SFSA

H. A. FORSBERG, Foundry & Mill Machinery Division, Blaw Knox Company, Chairman

ROBERT D. AHLES, General Electric Company

H. H. BLOSJO, Malleable Iron Fittings Company

W. K. BOCK, National Malleable & Steel Castings Company

W. P. DUDLEY, The Ohio Steel Foundry Company

W. D. EMMETT, Los Angeles Steel Casting Company

A. P. GUIDI, Texas Foundries, Inc.

G. F. HAISLUP, Electric Steel Castings Company

CHARLES LOCKE, The Crucible Steel Casting Company

E. A. WALCHER, JR., American Steel Foundries

W. D. WALTHER, The Dayton Steel Foundry Company

V. E. ZANG, Unitcast Corporation

DIRECTOR OF RESEARCH AND JOURNAL EDITOR
CHARLES W. BRIGGS

EDITORIAL STAFF

R. A. WILLEY,
Assistant Technical
and Research Director

HAROLD G. FRAUNHOFER
AND
CHARLES A. ROWE,
Assistants to the Technical
and Research Director

© by Steel Founders' Society of America, 1960

606 Terminal Tower Cleveland 13, Ohio

THE CIRCULATION OF THE JOURNAL IS RESTRICTED TO MEMBERS OF THE SOCIETY AND OTHERS AS AUTHORIZED BY THE BOARD OF DIRECTORS

A MICROSCOPIC STUDY OF THE BONDING OF STEEL FOUNDRY SANDS BY CLAYS

by

J. B. Caine*, E. H. King and J. S. Schumacher*****

There are many references in the literature to "clay film thickness" and the effect of mulling on "clay distribution". A study of these references reveals that in most cases, a uniform distribution of the bond clay about the sand grain is assumed but not proven. Clay distribution in mulling studies is assumed to be improved when green strength increases. Green strength does increase with mulling up to a point, but this is no proof that distribution in itself has changed.

Foundry sand technology abounds with such basic, unproven assumptions which may or may not be correct. A microscopic study was made in an effort to check the two basic assumptions of the previous paragraph. It should be emphasized that the findings reported in this paper merely present the problem, and the reader should be warned not to jump to further conclusions which have not been proven. The problem is too important and too basic to compound present confusion by more assumptions not based on fact. This particular investigation is restricted to steel foundry sands, for such sands constitute the great majority of the sands studied. However, there seems no reason why the basic findings cannot be extended to all foundry sands. The microscopic examination of sand requires different techniques than for metal. A detailed explanation of these techniques is in order for the proper interpretation of the photomicrographs to follow.

Sand grains and their coatings can be studied by oblique illumination as in Figure 1. Such illumination is ideal for uncoated grains, but does not show too much as to the coating, especially its thickness and distribution. Angular transmitted illumination, as in Figure 2, gives a shadow picture of the relative amount, thickness and distribution of the bond coating. Normal transmitted illumination, as is standard with the biological microscope, does not seem as good as the angular transmitted illumination of Figure 2, in that the main light beam focused directly into the objective lens and unimpeded through the spaces between the loose sand grains blinds the viewer, or causes excessive photographic contrast. A study of loose, individual sand grains is restricted to magnifications less than 30 diameters (30X) because of the very short depth of focus at higher magnifications.

* Consultant, Cincinnati, Ohio, ** President and *** Vice President, Hill and Griffith Co., Cincinnati, Ohio.

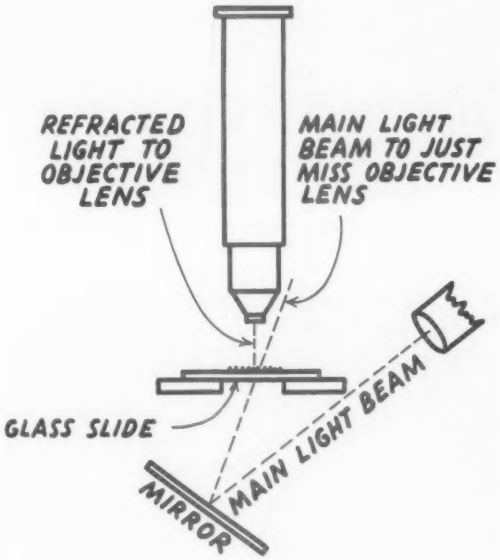

Figure 1—Angular transmitted illumination.

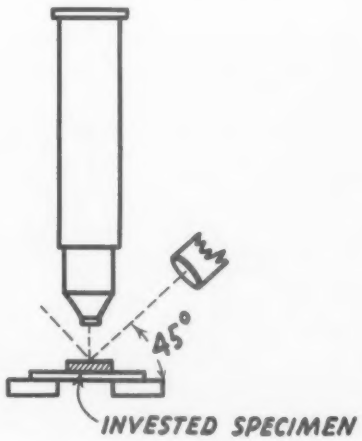

Figure 2—Oblique illumination.

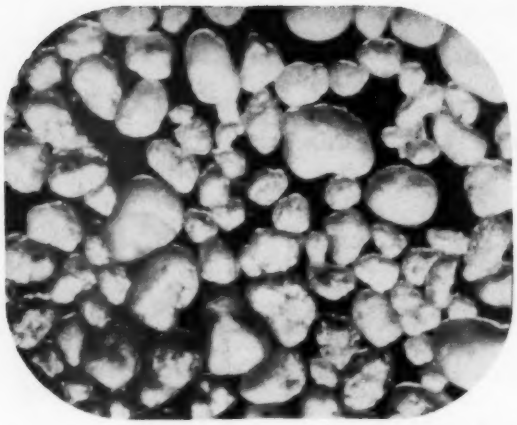

Figure 3a—Washed Ottawa type sand unbonded. 25X. Oblique illumination.

Figure 3b—Same as 3a, but bonded with 6% western bentonite. 25X. Oblique illumination.

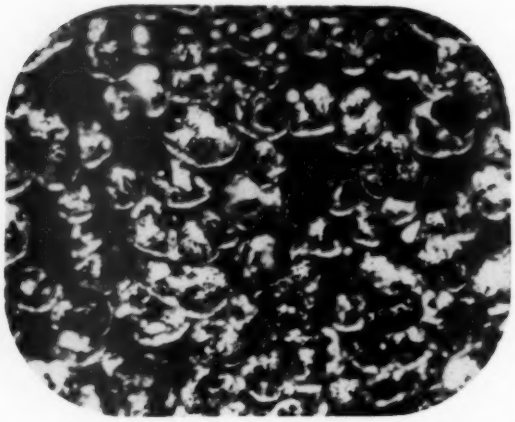

Figure 3c—Same as 3b, 6% western bentonite, but using angular transmitted illumination. 25X.

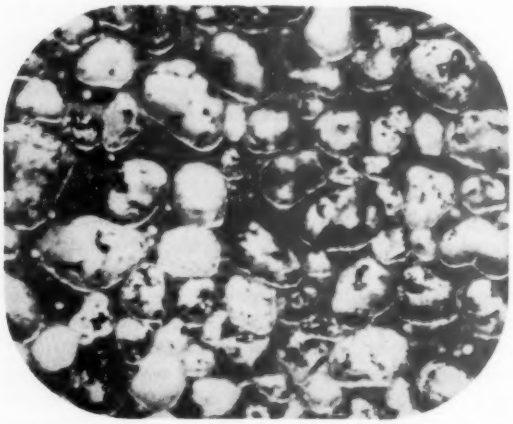

Figure 3d—Same sand as 3a and b, after dry reclamation to 3% AFS clay. 25X. Angular transmitted illumination.

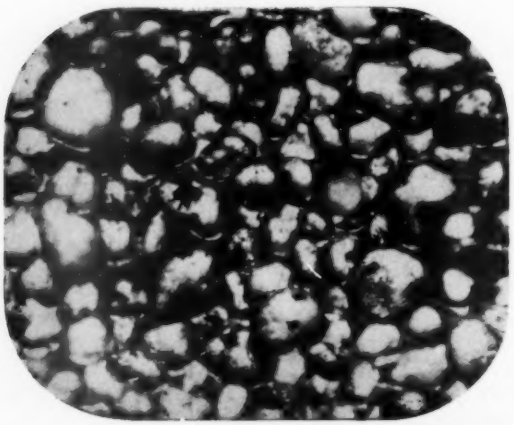

Figure 3e—Same sand as 3a, b, c, after clay removed by AFS washing method. 25X. Angular transmitted illumination.

The sand distribution of a compact must be preserved, therefore, rammed sand compacts require different preparation than individual sand grains. This can be done by carefully investing the compact in a thermosetting plastic. Phenol resin core binder rendered opaque with a little lampblack is handy for the foundry, for these materials are available in most core rooms and pattern shops. The resin is set at as low a temperature as possible to prevent bubbles. This usually requires 24 hours at under 200 degrees F. The specimen is then polished just like a metal specimen. Vertical illumination shows little, so oblique illumination is used. Such illumination restricts magnification to about 250X with a 4mm objective. Sufficient light is difficult to transmit to objectives of shorter focal length.

The technique used in other fields of examining thin sections by transmitted light has not been used because of the lack of equipment for specimen preparation. It is not known if such specimens will tell more than those used in this study.

Figure 3 shows a series of sand photomicrographs used to "zero in" the study of individual sand grains. Figure 3a shows the sand unbonded and is typical of many shown in the past. Figure 3b shows the same sand bonded with 6 percent western bentonite to which a pinch of lampblack was added for photographic contrast. Oblique illumination was used. At first glance, the grains seem uniformly coated, but on close examination irregularities can be seen. Transmitted light, as in Figure 3c, shows a different picture. The light areas on the sand grains have a very thin coating of bentonite or none at all. Most of the bentonite is concentrated in spots, or rings. If Figure 3c is believed, it is necessary to revise the whole thinking about clay coatings on sand grains. There is no such thing as "clay film thickness". Instead, a nonuniform coating seems to be a basic premise. It must be emphasized that Figure 3c is not a freak. It is representative of several hundred specimens.

Figure 3d is a further effort to "zero in" the technique. It shows the same sand after dry reclamation to 3 percent AFS clay. The decrease in amount of coating is apparent. Figure 3e shows the same sand after the standard washing to remove clay. Only that in pits remains.

It should be emphasized that the light and dark areas of Figure 3c and those to follow do not designate areas of clay and no clay. Figure 3b shows that there is a coating over the whole grain. The light and dark areas shown by angular transmitted light only designate areas of varying clay film thickness. Photomicrographs shown later, especially Figure 13, indicate that the dark areas correspond to clay film thicknesses of the order of 0.0005 inch. The clay films on the light areas cannot be seen on cross section at 250X and are probably in the order of 0.00005 inch thick, or less. A basic question that cannot be answered at this time is how thick must the bond film be in order to bond two spherical particles.

Figures 4 and 5 show sands after two mulling cycles in two types of mullers. Microscopic studies to date show little difference in clay distribution during the usual mulling cycles of the steel foundry. Either slight differences in distribution of the coating on the sand grains are significant, or other explanations are necessary for the changes in properties due to mulling. Mulling is usually evaluated by green strength. It has been the assumption that green strength is related to bond dispersion and that increased dispersion of the bond results in increased green strength. Figures 4 and 5 cast doubt on this basic assumption.

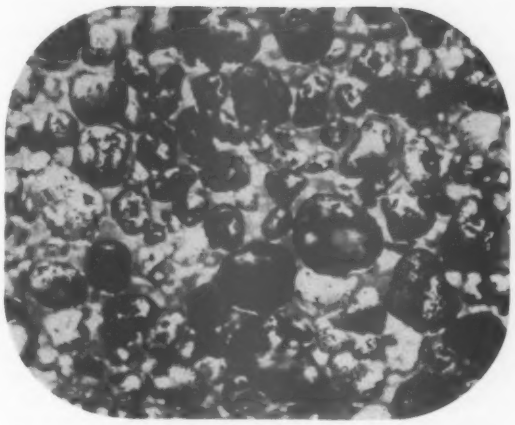

Figure 4a—Sand with 6% western bentonite added, mulled 1 minute in a slow speed muller. 25X. Angular transmitted illumination.

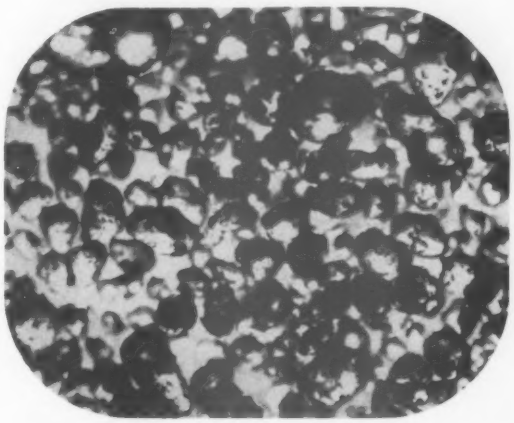

Figure 4b—Same sand, mulled 6 minutes in a slow speed muller. 25X. Angular transmitted illumination.

There is at least one other possible explanation for the variation in mechanical properties of the sand due to mulling, that is, changes in the bond itself. Mulling "plasticizes" all clays by developing strength, adhesion and cohesion. It is just as probable that the plasticizing of the clay is responsible for the increase in green strength, deformation and dry strength, rather than that the increased properties are the result of an unobservable increase in dispersion of the clay.

Mulling to maximum values of green strength and deformation may be detrimental in view of the fact that flowability or moldability of any clay-bonded sand decreases with increased green strength. Only a minimum green strength is required for mechanical strength during molding. Any excess green strength, as distinguished from green strength as a measure of clay content for thermal stability, is a disadvantage.

Similar conditions exist for deformation. Only a minimum deformation is required to prevent cracking and sticking during molding due to misalignment. Unless deformation is a measure of some phase of thermal stability, any excess is a disadvantage in decreasing flowability.

Dry strength is another property that is increased by mulling. Also, dry strength may likewise be related to certain phases of thermal stability. If this is true, there are ways to increase dry strength other than mulling and retain moldability. One way is to slightly increase the water content and shorten the mulling cycle.

However, slight variations in water content in themselves do not seem to change clay distribution greatly. A number of sands were mulled in the laboratory with water contents from 2 to 25 percent

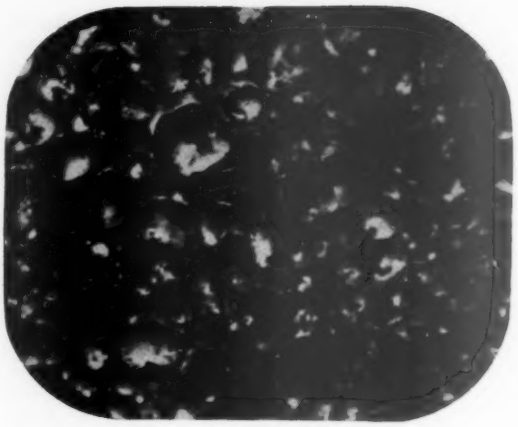

Figure 6a—New sand, 12% western bentonite, 8% water. 25X. Angular transmitted illumination.

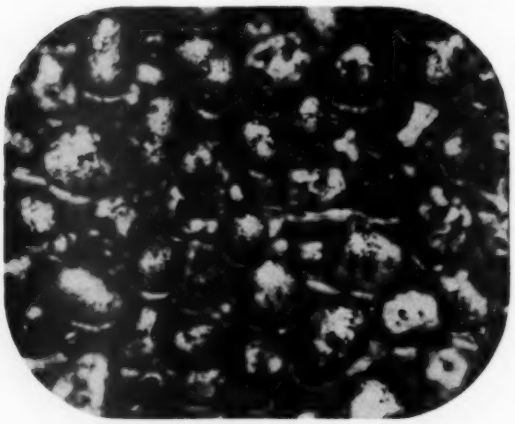

Figure 5a—Sand with 6% western bentonite added, mulled 20 seconds in high speed muller. 25X. Angular transmitted illumination.

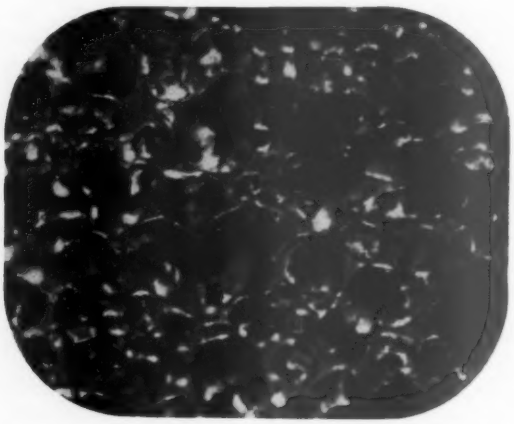

Figure 6b—New sand, 18% western bentonite, 6% water. 25X. Angular transmitted illumination.

Figure 5b—Same sand mulled 60 seconds in high speed muller. 25X. Angular transmitted illumination.

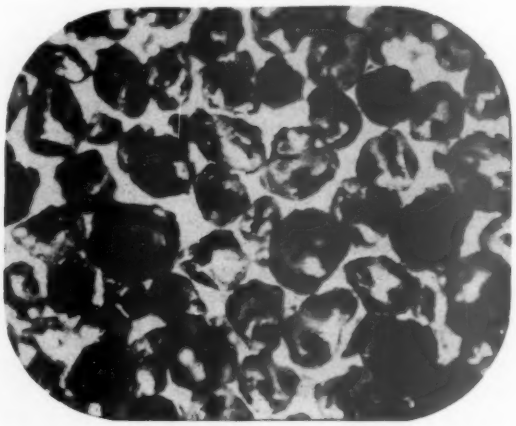

Figure 6c—New sand, 18% Ohio fire clay, 6% water. 25X. Angular transmitted illumination.

with 6 percent bentonite. There was no increase in dispersion over that of Figures 3 and 5 as the water was increased from 2 to 15 percent.

However, a definite increase in dispersion was found over 20 percent water, but these sands were not moldable. They were no longer molding sands, but approached slurries.

Only two methods have been found to date to approach uniform coating of sand grains with clay: (1) high clay content, and (2) reuse of the sand in the foundry. Figure 6 shows that 12 to 18 percent western bentonite almost covers the sand grains. Figure 6c shows about the same amount of coating with Ohio fire clay. Reuse of sand is restricted in the steel foundry due to danger of scabbing, but the point is interesting. Figure 7 shows the sand from one steel foundry using a very minimum of new sand. An appreciable number of grains are completely covered. Figure 8a shows a system sand, used in an iron foundry, whose grains are almost completely covered.

The assumption should not be made at present that it is desirable to have uniformly covered sand grains in the steel foundry. Other factors must be taken into consideration. For example, the steel sand of Figure 7 does not make particularly good castings, in fact, they could be classed as below average. Figure 8b shows the iron sand of Figure 8a after investing with plastic, polishing and at higher magnification. The loose shell around one sand grain is evident. This sand makes excellent iron castings, but such loosely bonded sand grains can be suspected as one reason why steel sands fail on continued reuse without reclamation.

Figure 8b introduces the second microscopic technique for sands, that of examining rammed sand compacts, invested with a mounting medium and studied at relatively high magnification. A fundamental point here is the identification of the phases. There is little doubt of the silica grain of Figure 8b and that this silica grain is surrounded by a relatively thick coating of another phase. It seems safe to assume that the surrounding phase is nongranular in the sense that the silica grain is granular. The main nongranular materials present in this sand are western bentonite and sea coal from the additions. This bentonite and sea coal would be dehydrated and charred from heating during reuse. The "coky" appearance of the shell of Figure 8b is typical of reused sands. The coky appearance of the coating of Figure 8b is different than the appearance of fine silica particles, as the silica flour particles of Figure 9.

Figure 10 is shown as the basis of comparison for the evaluation of bond coatings at high magnification on unbonded, white silica sand. This specimen was vibrated in a test tube to 61 percent density, invested, solidified and the test tube broken away from the specimen. Note the chains of white refraction dots around the sand grains. These dots, at present,

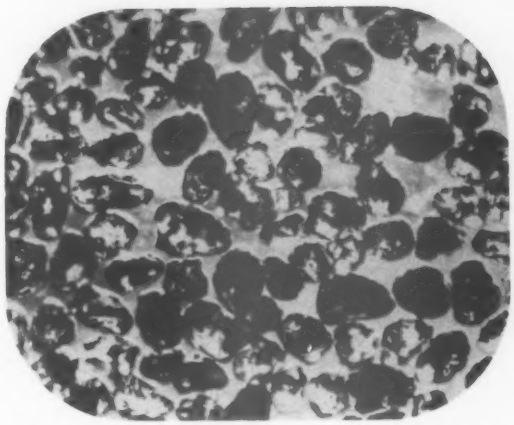

Figure 7—Steel system sand, 8psi green strength, 10% AFS clay. 25X. Angular transmitted illumination.

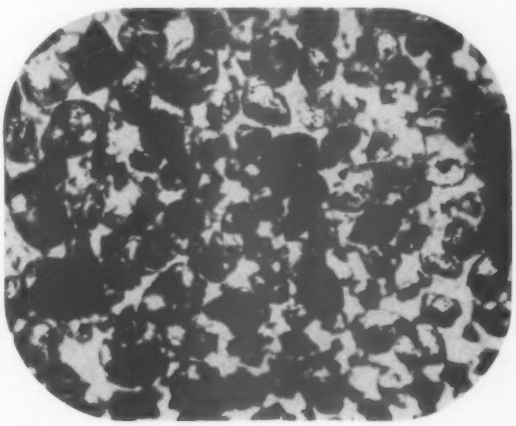

Figure 8a—Iron system sand. 26 psi green strength, 17% AFS clay, 5.1% loss on ignition. 25X. Angular transmitted illumination.

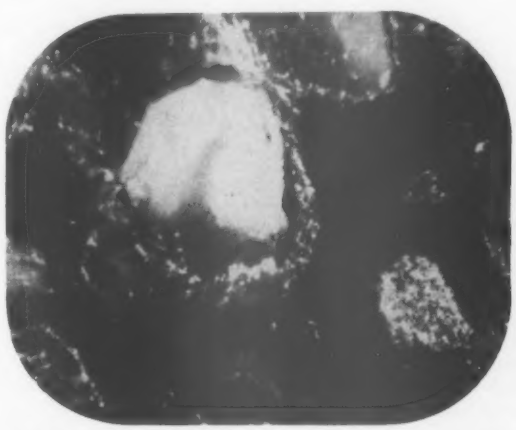

Figure 8b—Same as 8a, but at 125X. Invested and polished. Oblique illumination.

Figure 9—New steel core sand containing 25% silica flour. 125X. Invested and polished. Oblique illumination.

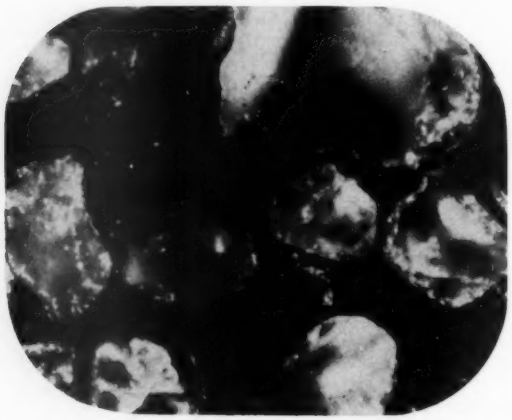

Figure 10—Washed, unbonded sand. 125X. Invested and polished. Oblique illumination.

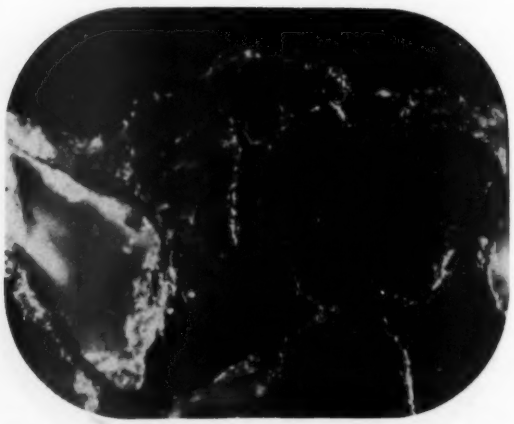

Figure 11—Surface coated with western bentonite slurry to distinguished bentonite. 125X. Invested and polished. Oblique illumination.

Figure 12—Coating obtained with 18% Ohio fire clay. 125X. Invested and polished. Oblique illumination.

interfere with the evaluation of very small amounts of bond coatings. The white refraction dots of Figure 10 must sometimes be used as sort of a blank in the evaluation of thin bond coatings.

Figure 11 is an attempt to establish the appearance of western bentonite at relatively high magnification. It shows a coating of western bentonite along the top, horizontal surface made by dipping a sand specimen in a bentonite slurry. The bentonite appears "pearly" under visual examination. A normal bonded contact between two sand grains is seen in the lower, right, center of Figure 11. Figure 12 illustrates a relatively thick bond coating, formed in this instance by 18 percent Ohio fire clay. The fireclay does not seem as translucent as western bentonite, but the difference is slight.

Figure 13 illustrates the appearance of what are now considered normal bentonite coatings, 6 to 8 percent, at successively higher magnification. These are production steel facing sands. Note the bond at the grain contacts. Figure 13b shows bond at the grain contact, a gap and a spot of bentonite away from the contact. It should be emphasized that areas showing bond contacts are not easy to find under the microscope. This may, or may not be as it should. First, the examination of a single plane through a three dimensional mass cannot be used, except statistically, as a criterion of the mass. Perhaps particles that do not seem bonded on a single plane are bonded on a different plane. Then too, the nonuniform coating makes it improbable that every contact point will be bonded.

This last point indicates that a uniform coating may be an advantage. This is probable, but for one point. There is the possibility of two grains sliding against their unbonded surfaces during ramming until they hit a spot of bond. If this action could be

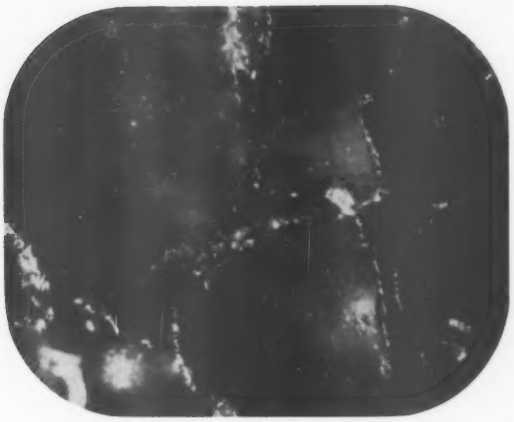

Figure 13a—Production steel facing sand. 8% bentonite. 125X. Clay areas 0.00056" thick.

Figure 13b—Production steel facing. 8% bentonite. 250X. Clay areas 0.0005" thick.

relied upon, it would enhance flowability and moldability without sacrifice of bonding. These points can be studied and evaluated quantitatively if done statistically. However, the study quickly becomes quite complicated, complicated to the point of order-disorder mechanics of atomic physics.

Summary

This report by necessity and by intention raises more questions than it answers. It has been released chiefly to give pause to some current thinking. Another reason for its release is to create interest and possibly help. The results to date can be summarized as follows:

1. The theories of uniform distribution of a clay substance on sand grains and "clay film thickness", within the ranges of clay content and water used in the steel foundry, are possibly in error. All that can be hoped for with present bonding techniques is a varying degree of nonuniformity.

2. Mulling over quite short intervals of time does not increase "clay distribution" as evaluated by this work. The increase in green and dry strength with increased mulling may not primarily be due to improved distribution of the bond. The increase in green strength may be detrimental in that moldability is decreased. The role of dry strength is not known.

3. Techniques of specimen preparation for microscopic examination are given. Preliminary qualitative methods for differentiation of the various bond constituents are given.

GRAIN OF SOLIDIFYING METAL REFINED BY VIBRATION*

by

I. I. Novikov, G. A. Korol'kov, V. V. Solov'eva, and A. Freilikh

Considerable attention has been paid to the refinement of the macrostructure of castings and ingots during solidification under the influence of vibration[1,2,3,4]. In almost all studies in which the frequencies used have not been above sonic, vibrations from mechanical, pneumatic or electromagnetic vibrators have been transferred directly not to the liquid metal, but to the mold (ingot mold, chill or sand mold). The mold itself, the solidified metal skin, the metal in the solid-liquid state and the liquid metal were set in vibration. There is a description of the effect of vibration on the macrostructure of the solidifying metal[2], as well as of the usual experiments on vibration of molds. To communicate virbrations directly to the melt, a silica rod of 3/8 inch diameter was introduced 1 inch deep into the metal. A specially constructed furnace ensured that the casting, 11/16 inch in diameter and 5-7/8 inches high, solidified from the bottom upward. The silica rod was set in vibration at 60 and 900 cps by an electromagnetic vibrator. It was concluded that vibrating the melt does not appreciably refine the grain of aluminum alloys, whereas vibrating a metal mold greatly refines the macrostructure.

*Translated from *Liteinoe Proizvodstvo*, Feb. 1959, No. 2, page 42.

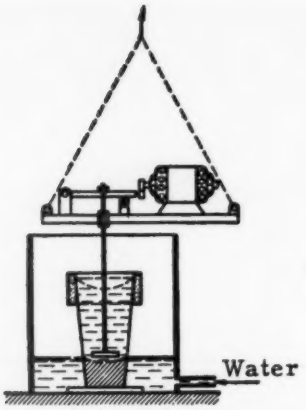

Figure 1—Mechanical vibrator setup.

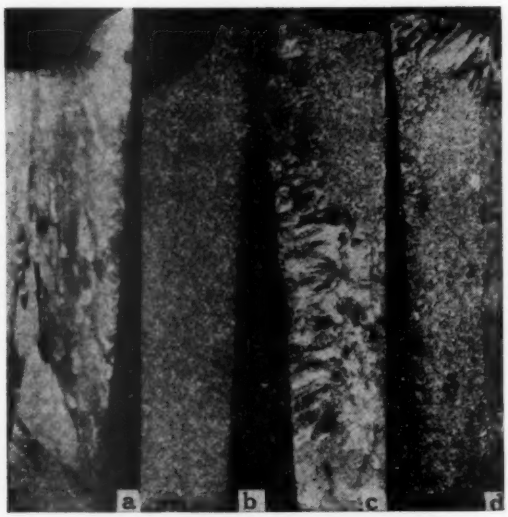

Figure 2—Various macrostructures observed.

The effect of vibrations of comparatively low frequency on the structure of a metal is of practical interest. For instance, to refine the grain of semi-continuously cast billets, the liquid metal in the cavity may be set vibrating. In this connection, it is necessary to find out whether it is at all possible to refine the structure by injection of low frequency vibrations.

A mechanical vibrator was used, similar to that described by Novikov et al[5]. To the vibrator stand a rod was fixed, carrying a disk at its end, immersed in the metal (Figure 1). The disk vibrated at 120 cps with an amplitude of 0.0071 inch. To prevent the disk from becoming enclosed on all sides by solidified metal, directional solidification had to be ensured. For this purpose a cylindrical steel mold, diameter 3.55 inches, height 11.8 inches and wall thickness 3/64 inch, was placed in the middle of a tank. After metal had been run into the stationary mold, water was admitted to the tank at a rate such that its level rose at 6-3/4 inches per minute. The upper part of the mold was surrounded by a hot top and as the water rose in the tank, the metal in the mold solidified from the bottom upwards. The disk of the vibrator, at the moment when pouring of metal ceased, was approximately at the bottom of the mold. As the level of water in the tank rose, the vibration rig was raised, so that the distance between the vibrating disk and the solidification front remained approximately constant.

Experiments showed that in all cases vibration of the melt close to the solidification front refines the metal microstructure considerably. Figure 2a shows the structure of a technically pure aluminum ingot, solidified without vibration, and Figure 2b with vibration close to the solidification front.

If vibration is stopped when the solidification front is a certain distance from the open surface of the melt, a coarse-grained zone is discovered in the upper part of the ingot (Figure 2d). It is characteristic that the boundary between the zones of coarse and fine grain is very sharp and comes at the height of mold at which vibration was stopped.

If the vibrating disk is in the upper part of the mold right from the start, there is practically no refinement of the grain in the lower part of the mold (Figure 2c). Even if the disk vibrates during the whole period of directional solidification, the boundary between the fine and coarse grained zones remains very sharp. Evidently effective grain refinement in this experiment starts only when the rising solidification front comes close to the vibrating disk. The lack of success in securing refinement, reported in reference 2, may be explained by the fact that in those experiments the vibrating rod was in the upper part of the melt, far from the solidification front.

Hence, vibration of a melt close to the solidification front, like vibration of a mold, refines the macrostructure and eliminates columnar crystallization.

References

1. D. K. Chernov, ZAP. RUSS. TEKH. OBSHCH, No. 7, 1868.
2. W. Rostoker and M. I. Berger, FOUNDRY, vol. 81, No. 7.
3. V. M. Govorkov and K. N. Shablin, ZHUR. TEKH. FIZ., vol. 24, No. 1, 1953.
4. D. W. Levinson, A. H. Murphy and W. Rostoker, LIGHT METAL AGE, 1950, Nos. 3-4.
5. I. I. Novikov, G. A. Korol'kov and A. E. Semenov, LIT. PROIZVODSTOVO, 1953, (1), 7-8. [Brutcher Translation No. 4596].

THE SOLIDIFICATION OF STEEL CASTINGS

by

H. G. Fraunhofer† and C. A. Rowe†

Contained herein is Part I of an up-to-date and extensive review of the literature on the subject of solidification of steel castings. This presentation discusses basic aspects of solidification of metals and unique aspects characteristic of steel solidification. Part II, which will appear in the next issue of the Journal of Steel Castings Research, will discuss the effect on solidification of such factors as mold materials, chills, gravity, convection, etc. A discussion of the solidification times for steel castings of various shapes will also be included.

INTRODUCTION

Extensive information is now available in the literature on the mode of the solidification of steel castings. However, this information is not being used to its greatest advantage, primarily because it is dispersed throughout the literature under various subjects, such as risering, chilling, shrinkage, etc.

This presentation is an attempt to collect and collate all the available literature on the solidification of steel castings, beginning with a discussion of the basic aspects of solidification applicable to metals in general. Unique aspects and characteristics of steel solidification are then discussed, followed by comments concerning the factors affecting the solidification process and solidification times of steel castings. No direct mention is made of such related subjects as risering or gating of steel castings, or solidification of steel in ingot form.

BASIC ASPECTS OF SOLIDIFICATION

Nuclei and Dendrite Formation

The solidification of steel begins in a manner similar to that of nearly every metal, namely, with the formation of nuclei. Submicroscopic particles, or nuclei, of solid metal begin to form at various places throughout the melt when the molten metal cools to the freezing temperature. These nuclei grow in size as time proceeds, and additional solid nuclei form throughout the melt. The growth of nuclei takes place according to a definite geometric pattern. This pattern, shown in Figure 1, takes on the form of a microscopic dendrite skeleton with regularly spaced branches and sub-branches placed at right angles to one another.

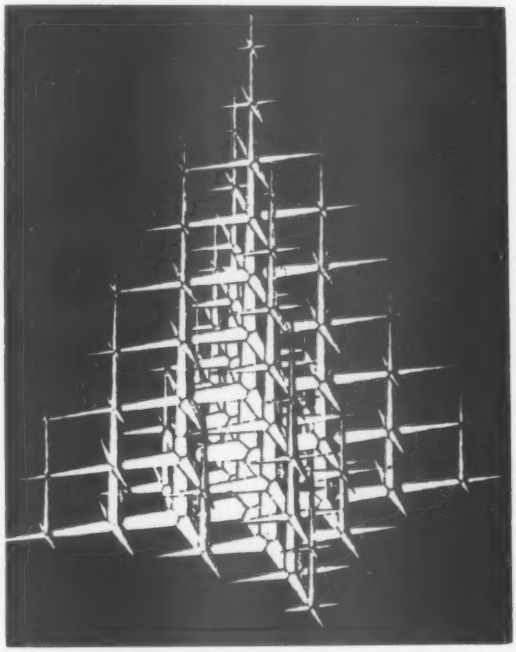

Figure 1—Schematic drawing of the growth of a dendrite from liquid. (After Bishop and Pellini)[1]

As solidification continues, the branches of the dendrite not only spread out into the liquid but also grow in thickness until the hollow spaces in the skeleton are solidly filled. In this manner, the dendritic growth of a crystal takes place. The spreading of the branches to increase the size of this crystal must eventually come to a stop, resulting from the growing together of the crystal and other nearby crystals. All crystals grow in this dendritic manner, no matter what their final shape or size may be. This process converts all the liquid to solid and constitutes what is called the freezing of the casting.

†Assistants to the Technical and Research Director, Steel Founders' Society of America

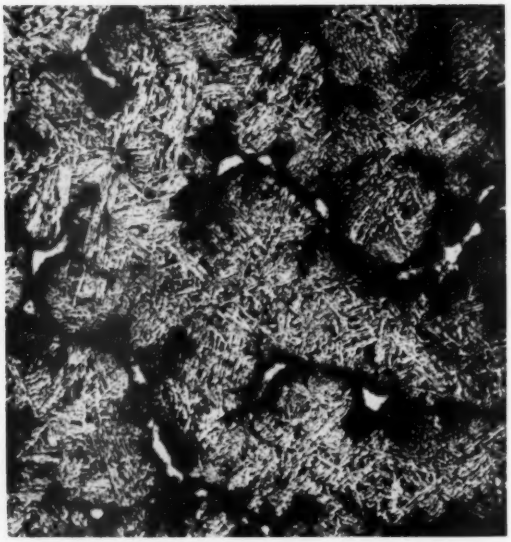

Figure 2—As-cast microstructure of a 4340 cast steel showing the dendrites present in the microstructure. Magnification 50x; nital etch.

These dendrites, which form from the melt, can often be seen in the microstructure of the solid casting by differential etching. Figure 2 is a photomicrograph of the as-cast microstructure of a 4340 cast steel. The dendrites are clearly outlined because of the coring, or microsegregation, which has occurred during solidification. A long heat treating cycle, including a homogenizing treatment, has very little effect upon the coring shown here.

The distribution of the nuclei which form from the melt is not entirely a random one. When steel is poured into a mold and allowed to solidify, the first nuclei originate in contact with the walls of the mold, since it is here that the temperature first falls low enough for their formation. The numerous nuclei at the mold-metal interface prevent individual nucleus growth in any but one direction, inward, and comparatively few of these grow to such a size as to penetrate far into the molten metal.

The formation and growth of crystals are determined by the temperature distribution in the casting. The temperature distribution in the mold and the casting after a given time is illustrated in Figure 3. This illustration shows that if molten metal is poured against a flat mold face, heat will flow into the mold and a solid layer of metal will be deposited at the mold-metal interface. The thickness of this layer will increase with time as heat continues to flow outward. The temperature of the boundary between liquid and solid metal is, of course, the freezing point of the metal, and heat of solidification is liberated at this boundary. The rate at which the boundary moves is determined by how rapidly the heat of fusion is removed.

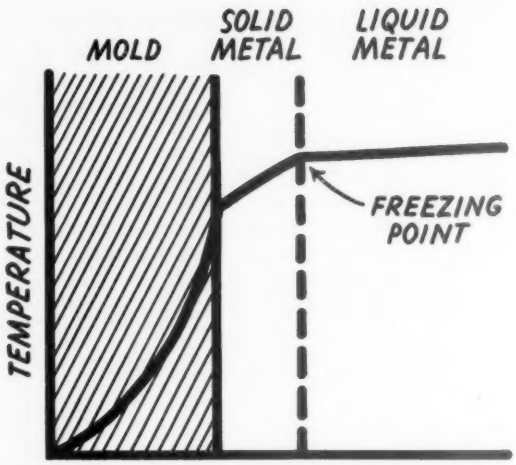

Figure 3—Temperature distribution showing heat flow during unidirectional solidification of a pure metal from a flat mold wall.

The first stage in the solidification of a casting is the formation of a thin chill layer, owing to the low temperature of the mold. The chill layer usually possesses a finely grained structure, caused by the rapid cooling and large number of nuclei which form. The chill layer, however, may entirely or partially disappear when very hot steel is used or when the mold is heated, reducing the chilling action of the mold. Dendrites start to grow from the inner boundary of the chill layer toward the thermal center of the mold. The resultant crystals will necessarily be elongated, or columnar, under usual conditions, for dendritic growth is preferential in the direction of the temperature gradient. Their direction thus indicates the direction in which a casting solidifies. As the growing columnar crystals approach the interior of the casting, the thermal gradient is diminished by the dissipation of superheat. This enables other crystals to nucleate at random rather than having continued growth take place at the tips of the columnar grains. This process is illustrated schematically in Figure 4.

Start and End of Freeze Waves

Commercial metals, in general, do not freeze at a definite, fixed melting point. Rather, they freeze over a range of temperatures which can be predicted from the phase diagram for the particular metal. Figure 5 illustrates schematically the relationship between the iron-carbon phase diagram and the mode of solidification of a 0.30 percent carbon steel casting. This diagram shows that because of thermal gradients which are active in the solidification of a casting from a mold wall there may exist: (1) a completely solid zone, (2) a zone consisting of solid dendrites with liquid metal at the dendrite interstices, and (3) a completely liquid zone. At least two, and often three, of these zones exist concurrently during the wall growth of a casting, depending upon the type of metal, the mold material and stage of solidification.

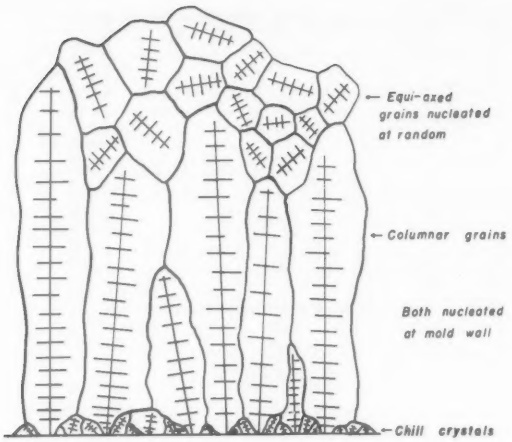

Figure 4—Schematic drawing of a cross section through a casting.

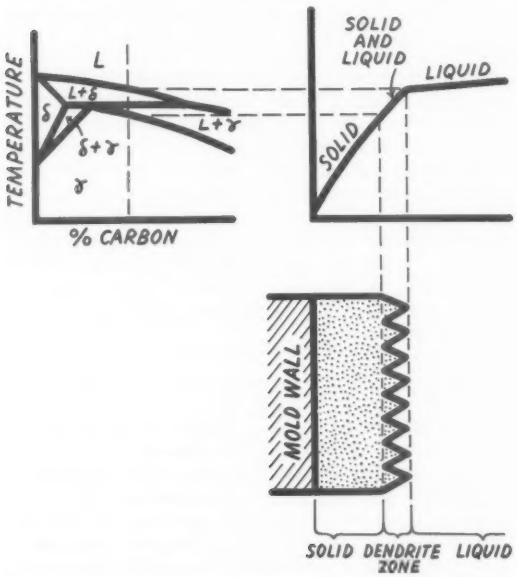

Figure 5—Diagram showing the relationship between the iron-carbon phase diagram and mode of solidification of a 0.30 percent carbon steel casting.

Wall growth may be visualized as occurring by the travel of two waves, the "start of freeze" and "end of freeze" waves, from the mold-metal interface to the casting center line. The start of freeze wave travels with the tips of the growing dendrites into free liquid and indicates the beginning of solidification. The end of freeze wave travels with the base of the growing dendrites where the last remaining liquid solidifies. The space separation between the two waves consists of intermixed liquid and solid metal and is the zone where actual solidification occurs.

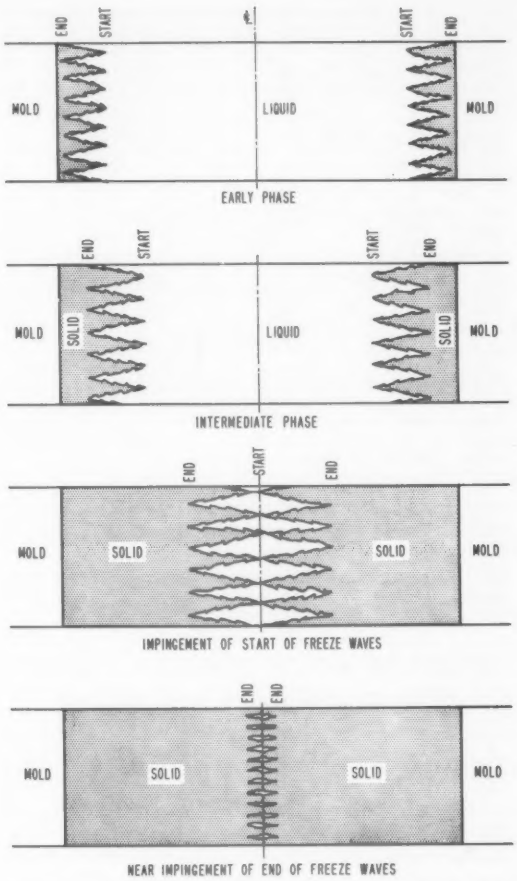

Figure 6—Mechanism of wall growth by progression of start and end of freeze waves. (Bishop and Pellini)[1]

Figure 6 illustrates various steps in the progression of the two waves over the cross section of a casting. The start of freeze wave, during the early stage of solidification, has progressed into the casting for an appreciable distance and the end of freeze wave has barely started its traverse. At an intermediate phase of solidification, both waves have traveled farther into the liquid, and there is a definite layer of completely solid skin at the surface. The two waves continue to advance until the dendrites from opposite faces impinge, thus eliminating the completely liquid zone. The end of freeze waves continue until the center line of the casting is reached, at which time solidification is complete.

The rates of travel of the start and end of freeze waves and their space separation within the casting vary with the mold materials and the type of metal undergoing solidification. Basically, these variations arise from the difference in thermal properties of both the mold and solidifying metal which govern the

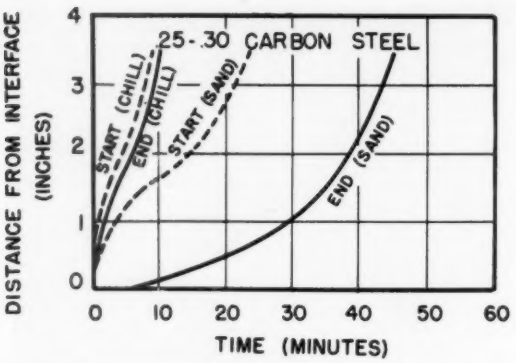

Figure 7—Start and end of freeze wave diagrams for a 0.25 - 0.30 percent carbon steel cast in a green sand and chill mold. Casting cross section 7 inches. Pouring temperature 2800 degrees F. Sand thickness 7 inches. Mold chill thickness 7⅛ inches. (Bishop and Pellini)[1]

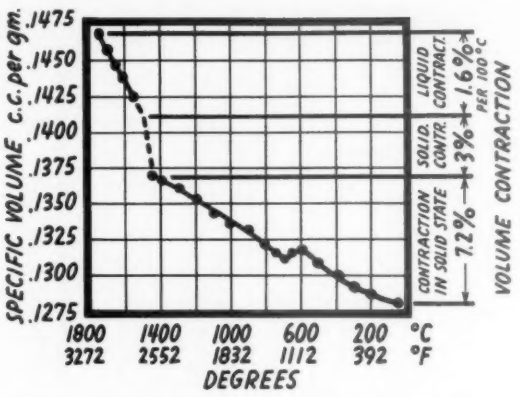

Figure 8—Volume change recorded on cooling of a 0.35 percent carbon cast steel. (Briggs and Gezelius)[2]

manner and rate of heat transfer. A typical start and end of freeze wave diagram is shown in Figure 7. This illustrates the mode of solidification of a 0.25 to 0.30 percent carbon steel in green sand and chill molds.

CHARACTERISTICS OF STEEL SOLIDIFICATION

Volume Changes During Solidification

The most obvious characteristic of the solidification process is the contraction or change in volume of the solidifying steel. This decrease in volume is an inherent characteristic of many solidifying metals. The total contraction of a steel casting is the sum of three stages: (1) liquid contraction; (2) solidification contraction; and (3) solid contraction. Figure 8 is a typical cooling curve for a carbon steel cooling from 1750 degrees C to room temperature. Total contraction has been found to increase with an increase in carbon content. What appears to be the most authoritative work on the subject[3], shows the change in specific volume of a 0.35 percent carbon steel expressed in terms of volume contraction at room temperature to be 1.6 percent per 100 degrees C or 0.89 percent per 100 degrees F. This value is slightly diminished by an increase of chromium and aluminum and increased by greater amounts of carbon, silicon, manganese and phosphorus. However, for the usual cast carbon steels and low-alloy cast steels, the liquid contraction may be considered to be about 1.50 to 1.75 percent of its volume at room temperature per 100 degrees C. This value is shown in Figure 8 in conjunction with solidification contraction and solid contraction.

Steel also contracts upon solidifying, i.e., as it passes through the two-phase, liquid plus solid region, and finally becomes completely solid. The various volume contraction figures which are available show an average of 0.0039 cc per gram for a 0.35 percent carbon steel which is equivalent to 2.85 percent of the specific volume of the solid steel at the freezing point, or 3.05 percent of the specific volume at room temperature.

There are no accurate measurements available of the effect on the solidifying contraction of such differences as may be encountered in the carbon and alloy contents in steels. However, it is believed that there would be but little change in the value with increasing carbon content since the specific volume of both liquid steel and solid steel increases as the carbon content is increased. Experimental evidence tends to show that pure iron exhibits a solidifying contraction of about 2.2 percent. This value increased to approximately 4 percent for that of a 1.00 percent carbon steel.

Equilibrium Phase Diagram

The iron-carbon phase diagram showing the liquidus and solidus curves is presented in Figure 9. It is noted that increased carbon content tends to lower both the solidus and liquidus and enlarge the freezing range. Slightly below and roughly paralleling these curves appear the liquidus and solidus curves which were obtained by a study of the melting and freezing temperatures of steel for commercial steel castings. In general, the curves for the commercial steel are situated about 20 to 25 degrees F below those of the iron-carbon system. However, the peritectic transformation occurring at 2718 degrees F does not appear to be altered in commercial cast steels.

A study[4] of the melting and freezing points of a number of commercial steels led to the conclusion that the liquidus and solidus curves of commercial carbon steels conform with the iron-carbon diagram with respect to carbon content and temperature, provided that the manganese content is below 0.45 percent and the silicon below 0.35 percent. However, if manganese and silicon contents are raised, the liquidus and solidus temperatures are lowered.

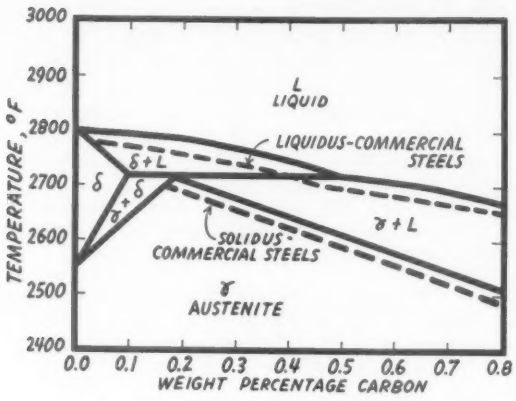

Figure 9—The iron-carbon phase diagram.

The dotted lines on the phase diagram of Figure 9 hold in general for steel castings of nickel and chromium content up to one percent.

The diagram of Figure 9 can be used to predict the freezing history of a steel cooled under equilibrium conditions. At 0.30 percent carbon commercial steel, for example, begins to freeze at 2740 degrees F with the formation of delta iron in the melt. At 2718 degrees F the steel will traverse the peritectic transformation and austenite will proceed to form directly from the melt. When the temperature drops to 2650 degrees F, the solidus is reached and freezing is complete.

Temperature Level and Temperature Range of Solidification

The equilibrium diagram of Figure 9 reveals a factor which has a significant influence on the mode of solidification of steel, specifically, the temperature level at which solidification occurs. Temperature gradients which are established between the solidifying metal and the mold wall are a function of the difference between the temperature of the metal and the temperature of the mold. The high solidification temperature of steel means a large temperature difference and thus steep thermal gradients which result in a high degree of progressive solidification.

The temperature range over which a metal solidifies, that is, in which liquid and solid phases coexist, is also an important factor in determining the mode of solidification. Steels containing 0.08, 0.25, and 0.60 percent carbon have been determined to solidify over a temperature range of 40, 75 and 125 degrees F, respectively. Given the same properties of the metal and the mold, and thus essentially the same temperature gradients, the steel with the narrowest solidification range will exhibit the highest degree of progressive solidification, since the gradients intercept the liquidus and solidus temperatures at more closely spaced locations. Thus, one would expect solidification to be highly progressive in a low carbon steel and much less progressive in medium and high carbon steels, and this is indeed the case, as may be seen in Figure 10. However, in all instances, the solidification is much more progressive than in nonferrous metals.

Thermal Conductivity of Mold and Solidifying Metal

The mode of solidification of a metal is a function of the thermal gradients established during freezing, therefore, the thermal properties of both the mold and the metal solidifying must be considered as important factors in the determination of the nature of steel solidification. A mold made of a material having a high thermal conductivity and a high heat capacity, such as a chill mold, will absorb heat quickly and over an extended period of time. A high conductivity also results in a rapid flow of heat away from the mold-metal interface which causes the interface of the solidifying metal and the mold to be maintained at relatively low temperatures. The low interface temperature means that steep thermal gradients will be established (Figure 11 (a)) and concomitantly solidification will be of a highly progressive nature.

The mode of solidification of metal in a sand mold will be quite different from that in a chill mold, due to the low thermal conductivity and low heat capacity. Sand, a good insulator, is able to absorb very little heat and is also unable to conduct heat away from the mold-metal interface at any appreciable rate. For this reason, the temperature of the sand at the casting interface approaches rapidly the temperature of the

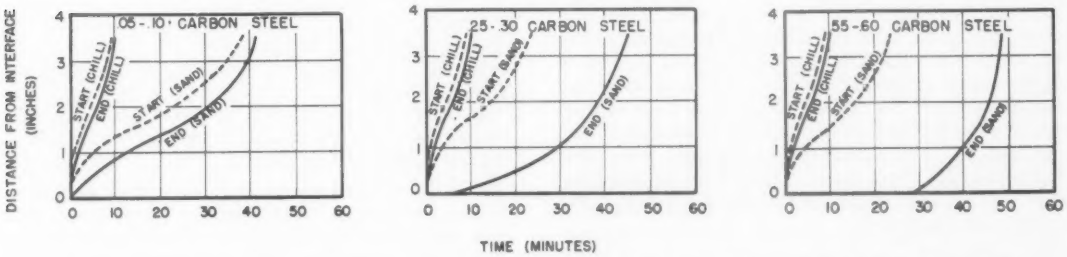

Figure 10—Effect of carbon content on the start and end of freeze waves in sand and chill molds. (Bishop and Pellini)[1]

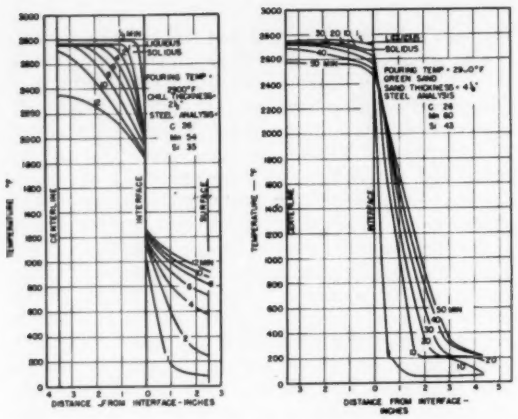

Figure 11—Thermal gradients in steel castings and in the mold; (a) 2½-inch thick chill used, (b) green sand—no chill. (Bishop and Pellini)[1]

solidifying metal (Figure 11 (b)) and only mild temperature gradients are established in the metal. Thus, metal poured into a sand mold will solidify in a much less progressive manner than in a chill mold.

The thermal conductivity of the freezing metal also exerts an appreciable effect on the thermal gradients established during solidification. A metal having a high conductivity will allow heat to be carried from the center of the solidifying section to the mold-metal interface very rapidly. Thus, heat removed by the mold from the casting surface will be quickly replaced by heat from the interior, and only mild gradients can exist within the freezing metal, causing poorly progressive solidification.

Heat flow within a solidifying metal having a low thermal conductivity is sluggish, thus allowing steep gradients to be formed and maintained, and solidification will be of a more progressive nature. Steel is a metal having a relatively low thermal conductivity, and this is one of the factors that aid in producing progressive solidification in the carbon grades having a wide temperature range of solidification. It should be pointed out that the effect of metal conductivity is minimized in a sand mold due to the low thermal conductivity of the sand.

To be continued in the next issue of the Journal of Steel Castings Research.

References

1. Bishop H. F., and Pellini, W. S., "Solidification of Metals", *Foundry* (February 1952), p. 86.

2. Briggs, C. W., and Gezelius, R. A., "Studies on Solidification and Contraction in Steel Castings, II - Free and Hindered Contraction of Alloy Cast Steel", *AFA Transactions,* Vol. 6 (June 1935), pp. 449-470.

3. Bendicks, C., Ericson, N., and Ericsson, G., "Bestimmung des spezifischen Volumes von Eisen, Nickel und Eisenlegierungen im geschmolzenen Zustand", *Archiv fuer das Eisenhuettenwessen* (January 1930), pp. 473-486.

4. Andrew, J. H., and Binnie, D., "The Liquidus and Solidus Ranges of Some Commercial Cast Steels", *The Journal of The Iron and Steel Institute,* Vol. 119 (1929), pp. 309-346.

A TESTING MACHINE FOR BLAST CLEANING ABRASIVES

by

P. Lambert*

A machine has been made for use in The British Steel Castings Research Association's current investigation into the efficiency of shot blasting methods. It is similar in design to one described by Bickel[1]; and a machine of essentially the same basic design, but incorporating many additional refinements, is marketed by G. Fischer, A. G., Schaffhausen. It is intended to test the cleaning efficiency and durability of different abrasives and the resulting wear on machine parts. The effects of blasting time, impact velocity and angle of impact can also be studied. The machine is a miniature blast cleaning plant and should provide, from tests of short duration, information which would normally require a prolonged test in full size equipment.

*The British Steel Castings Research Association, Plant Engineering Section

Figure 1 is a simplified arrangement drawing of the machine. The throwing wheel A gives the abrasive a velocity equal to that obtained in a full size plant at the face of the work. The "targets" B are steel blocks, presenting cast surfaces to the blast. Standard "Almen" test piece holders, designed to measure peening intensity, may be substituted for the steel blocks. Small particles are removed by the dust exhaust from the abrasive as it falls from the blasting chamber C through the exhaust ring D. The remainder of the material falls through the shutter E into the recirculating wheel F.

The 4-foot diameter recirculating wheel is of open channel section and is divided by partitions G into two compartments. As it rotates, the abrasive falling into it stays in the lower part, until a partition reaches the bottom position, when the abrasive is taken up

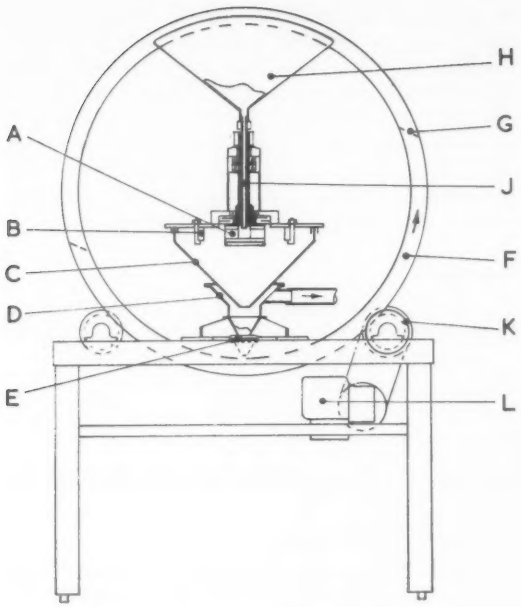

Figure 1—General arrangement of the shot testing machine.

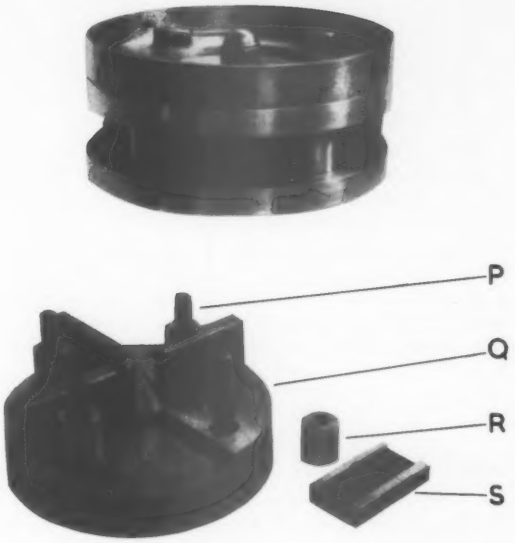

Figure 2—Abrasive throwing wheel.

and discharged into the hopper H. From here the abrasive falls down the feed tube J and into the throwing wheel A, when the cycle is repeated. The speed of the recirculating wheel is such that the whole of the charge is collected and dropped into the hopper H at once, ensuring that all particles complete an equal number of cycles of the test. The wheel is driven by friction between it and one of the two supporting rollers K. This roller is driven via stepped pulleys and a vee-belt by a ¼ h.p. geared motor L. Initially the wheel speed is 6 rev./min., but this is variable.

The abrasive throwing wheel (Figure 2) is of a 4⅞-inch diameter, i.e., one-quarter of the size of the 19½-inch diameter wheel normally used in blasting equipment. The four bolts P clamp the two side plates Q onto the bushings R, and the four blades S are held in slots in the inner faces of the side plates. The blades are retained in the slots by lugs, cast in the back, which locate on the bushings. Blades and side plates can be cast in any of the alloys used in these applications and are ready for assembly with the minimum of grinding. The four bolts hold the wheel assembly onto a boss at the lower end of the vertical spindle. This is mounted in ball and roller bearings and, initially, its speed is 9,000 rev./min. This can be varied by changing the motor pulley when the effects of varying impact velocity are studied. Drip-feed lubrication is provided for the spindle bearings and thrower rings keep oil in the bearings and abrasive out. A stationary feed tube, with a replaceable nozzle at the lower end, passes through the bore of the spindle and leads abrasive from the hopper at the top to the center of the throwing wheel. The spindle is driven by a 1 h.p., 2,880 rev./min. motor through a thin, flat plastic belt running on steel pulleys. The motor bracket is bolted to the spindle housing bracket through slots which allow movement for belt tension adjustment.

A steel pillar, with a baseplate bolted to the frame of the machine, supports the spindle and motor assembly. The lower flange of the spindle bearing housing carries a circular steel plate which holds the targets and forms the top of the blasting chamber. The targets can be fixed at any angle to the direction of the abrasive coming from the wheel. To the underside of the circular plate is attached a conical hopper which completes the blasting chamber, the small outlet hole at the bottom being surrounded by an annular chamber from which dust is extracted. Below this chamber a conical spout leads into the recirculating ring. The lower part of the blasting chamber is readily removed for changing targets and wheel assemblies.

An industrial vacuum cleaner is used to provide dust exhaust and separation of small particles of abrasive. The rate of air exhaust is adjustable, so that particles of any desired size can be separated; at present it is set at 15-20 cu.ft./min. to extract abrasive particles below about 0.010-inch diameter.

Two methods can be used to assess rate of breakdown of abrasive. One consists of comparing, for different abrasives, the number of cycles through the machine to cause a certain percentage loss of broken down abrasive to the dust exhaust. The other consists of running the abrasive through the machine

and making periodical additions to the sample to make up for the broken-down abrasive lost to the dust exhaust. The rates of replenishment for different abrasives are then compared and this method is nearer to conditions found in practice, although a longer time is needed for the test.

Rate of metal removal and other effects on the workpiece can be assessed by examination of the targets. Examination of the wheel parts will indicate the extent of wear on equipment.

During preliminary trials, 100-gram samples of chilled cast iron grit have shown appreciable breakdown after only 10 passages through the machine, while similar size samples of cast steel shot and cut-wire pellets have been passed through over 1,000 times without noticeable breakdown. Physical properties, such as hardness, chemical analysis, microstructure, etc., for samples of many abrasives have already been examined; and these properties will be compared with the performance of the samples in the testing machine. It is hoped that it may ultimately be possible to devise a simple test which can be carried out with normal laboratory equipment to indicate the quality of blast cleaning abrasives.

Reference

1. "Metallic Shot Blasting Material and Its Testing", by E. Bickel, *Stahl und Eisen,* 1956, 76 (17), 23rd August, 1116-1128.

ABSTRACTS OF FUNDAMENTAL PAPERS ON STEEL CASTING RESEARCH

Melting & Refining — Deoxidation

Sims, C. E., and Briggs, C. W., "A Primer on Deoxidation", JOURNAL OF METALS, December 1959. The why, what, and how of deoxidation are discussed in language which any steelmaker can understand. Various deoxidizers are discussed and evaluated.

Sands — Properties

Hofmann, Franz, "Modern Concepts on Clay Minerals for Foundry Sands", THE BRITISH FOUNDRYMAN, April 1959. The author discusses bonding capacity of various types of clay, the relation between green strength to actual behavior in production, evaluation of the optimum sodium carbonate addition, and the effect of heat, on bonding capacity of various bentonites.

Castings — Contraction Defects

Novikov, I. I., "Use of Vibrations During Solidification of Alloys to Eliminate Hot Tears", LITEINOE PROIZVODSTVO, January 1958, #1, Henry Brutcher, Technical Translations, No. 4753, P. O. Box 157, Altadena, Calif. Price $3.75. Investigation into effect of vibrations on hot tearing of alloys in process of solidifying. Influence of vibration frequency on development of hot tears; tears healed at subcritical vs. critical vibration frequencies.

Melting — Gases

Langenberg, F. C., and Snook, J. M., "Further Information on Sampling Liquid Steel for Dissolved Oxygen", Transactions of The Metallurgical Society of AIME, Vol. 215, August 1959. Information is given on simplified methods of determining oxygen content of the liquid steel bath. Advantages and disadvantages of the methods and their accuracy are discussed.

Castings — Solidification

Shtanko, D. A., "Use of a Rotating Magnetic Field in the Casting of Metals", ZHURNAL TEKHNICHESKOI FIZIKI, vol. 3, 1933, #7. Henry Brutcher, Technical Translations, No. 2126, P. O. Box 157, Altadena, Calif. Price $3.90. First report on experimental work on the solidification of metals (zinc, technical aluminum, aluminum bronze, and gray cast iron) in a rotating magnetic field.

Alloys — Corrosion and Heat Resistant

Kreshchanovskii, N. S., and Zabludovskii, I. E., "Effect of Inoculants on the Crystallization and Sulfur Distribution in Cast Austenitic Steel", METALLOW. TERM. OBRA. MET., March 1959, #3, 33 - 37, Henry Brutcher, Technical Translations, No. 4542, P. O. Box 157, Altadena, Calif. Price $3.50. Harmful effect of sulfur on properties of cast 15% Cr, 25% Ni steel. Study of distribution of sulfur by macro and microautoradiography; procedure; results. Compositions of steel, inoculated with 0.2% Zr or 0.3% Ce or 0.5% Ca, or uninoculated. Effect of Zr, Ce, and Ca on content and distribution of sulfur. Merits of treatment simultaneously with Ce and Ca.

Properties and Testing — General
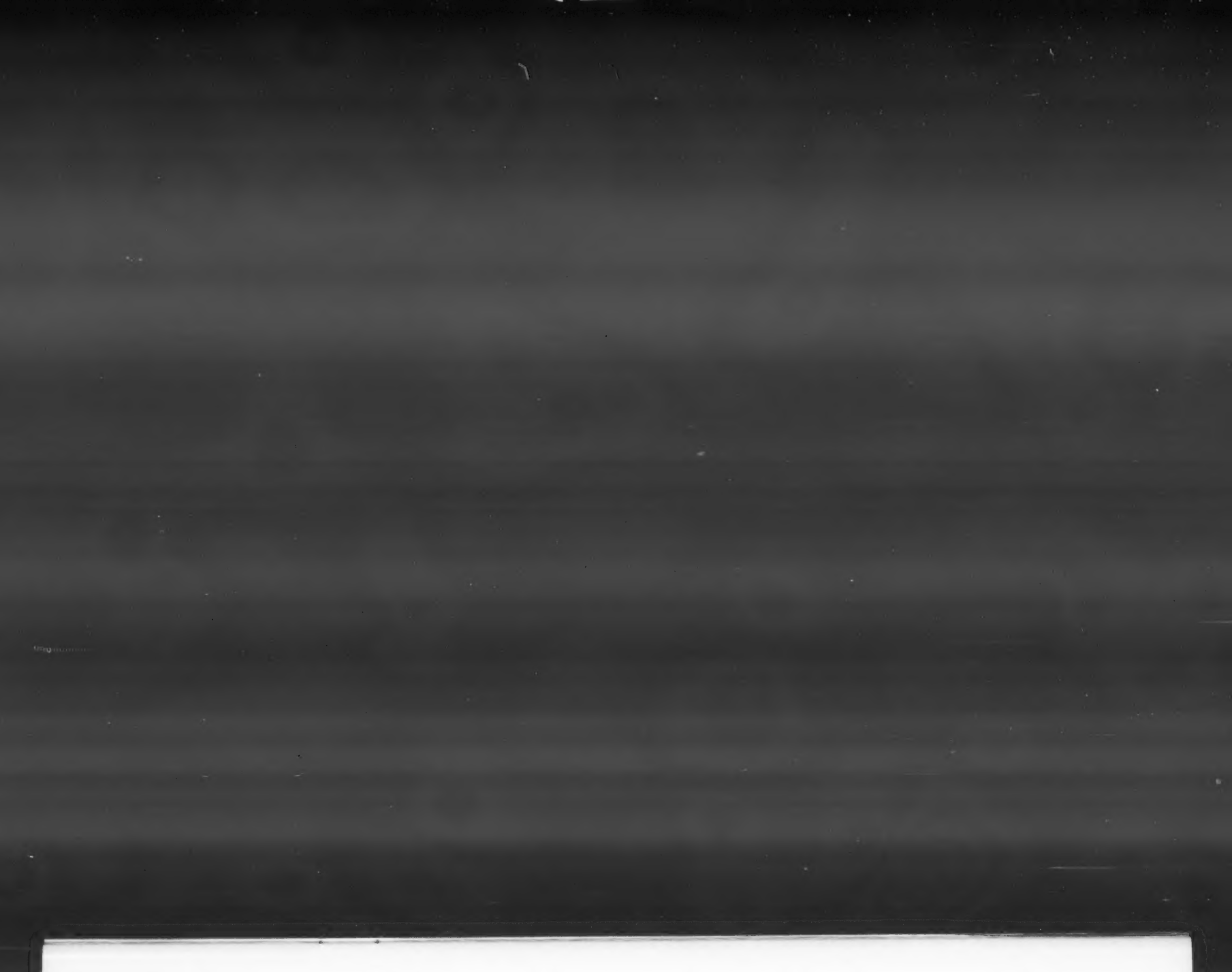
Niesse, J. E., Flemings, M. C., and Taylor, H. F., "Application of Theory in Understanding Fluidity of Metals", MODERN CASTINGS, November 1959. A theoretical analysis of fluidity of pure metals was carried out employing heat flow and fluid flow relationships. Equations were developed to predict fluidity of pure metals at their melting point and to predict the effect of superheat on fluidity. Experiments were made on fluidity of aluminum-tin alloys and on low-carbon steel.